npj | climate and atmospheric science

Article

Published in partnership with CECCR at King Abdulaziz University

https://doi.org/10.1038/s41612-024-00586-5

The impact of the Madden-Julian oscillation on spring and autumn afternoon diurnal convection in Sri Lanka

Check for updates

Wan-Ru Huang [1] ✉, Suranjith Bandara Koralegedara [1], Tzu-Yang Chiang[1], Cheng-An Lee[1], Po-Han Tung[1], Yu-Tang Chien [1] & Liping Deng [2]

This study examines the impact of strong Madden-Julian Oscillation (MJO) phases (P1–P8) on diurnal rainfall patterns focusing on Afternoon Diurnal Convection (ADC) events in Sri Lanka during 2001–2020 spring and autumn. Daily mean rainfall increases (decreases) during the P2-to-P3 (P6-to-P7) MJO phases in both seasons, while the diurnal rainfall amplitude peaks during the P2-to-P3 (P8-to-P1) MJO phases in spring (autumn). ADC events also occur more frequently and intensely during MJO P2-to-P3 (P8-to-P1) in spring (autumn). The MJO's modulation of diurnal rainfall amplitude and ADC events is more apparent in autumn than in spring. Active MJO phases enhance the westward propagation of diurnal rainfall associated with ADC events, sustained by moisture flux convergence and enhanced upward motion. The prevailing mid-to-upper level easterly wind, combined with deep convection over Sri Lanka, contributes to a more pronounced westward propagation during the P2-to-P3 (P8-to-P1) phases for ADC events in spring (autumn).

The Madden-Julian Oscillation (MJO)[1,2] is a key intraseasonal mode in the tropical atmosphere[3,4]. It generally features a 30-to-90-day oscillation period with a gradual eastward movement of tropical convective activity, extending from the western Indian Ocean, passing over Sri Lanka, and dissipating beyond the dateline[5–8]. MJO events can impact weather and climate patterns in the tropical Indo-Pacific region[4,9–16], including Sri Lanka[17]. It was noted that during the MJO's active period over the tropical Indian Ocean, clouds tend to be primarily deep and widely organized, resulting in frequent and intensive convective activities[12,16,18,19].

The distinct phases of MJO propagation and their associated atmospheric thermodynamic changes not only affect extreme rainfall formation[13,20,21] but can also exert a substantial influence on diurnal rainfall variability in various regions, particularly in tropical islands[9–11,14–16,22]. Several studies[15,22–26] have emphasized the MJO's influence on the diurnal characteristics of convective rainfall and its subsequent offshore movement from tropical islands to the surrounding oceans. For instance, research has shown that during active (inactive) MJO phases, diurnal rainfall amplitudes over India generally increase (decrease)[3,15,23]. Similarly, studies over the Maritime Continent[22,27,28] reported enhanced (weakened) diurnal cycles of rainfall during active (inactive) MJO phases.

Regarding diurnal rainfall propagation, diverse impacts of MJO's influence are observed in different regions. Mishra et al.[29] reported that the diurnal convective systems developed along the east coast of India propagate in a north-west to south-east direction in summer, where the inactive MJO phases show weakened diurnal convection compared to active MJO phases over India and the Bay of Bengal. Prajwal et al.[15] found eastward diurnal rainfall propagation influenced by the MJO during summer over the Western Ghats, India. Conversely, Zhu et al.[26] observed westward diurnal rainfall propagation over Sumatra, Indonesia, in winter under MJO influence. Additionally, Ichikawa and Yasunari[30] connected diurnal rainfall propagation over Borneo, specifically towards the leeward side of the island, and large-scale low-level tropospheric winds associated with the MJO. These differences in the MJO's modulation of diurnal rainfall propagation direction across various regions[15,26,29,30] highlight how the MJO's influence on regional diurnal rainfall formation and propagation can vary with location and season.

Sri Lanka, situated in the Indian Ocean between South India and Sumatra (Fig. 1a), occupies a pivotal position within the propagation pathway of the MJO[17]. Analyzing rainfall variation in Sri Lanka is critical for understanding the MJO's influence on regional rainfall[17,20,31]. Earlier studies[17,20,31] have indicated that more intensive daily mean rainfall occurs over Sri Lanka when the active phase of MJO propagates into the Indian Ocean (i.e., in phase 2 and 3 denoted as P2-to-P3 hereafter; see Methods section for definition). Regarding diurnal rainfall variation, Huang et al.[31]

[1]Department of Earth Sciences, National Taiwan Normal University, Taipei, Taiwan. [2]College of Ocean and Meteorology, Guangdong Ocean University, Zhanjiang, China. ✉e-mail: wrhuang@ntnu.edu.tw

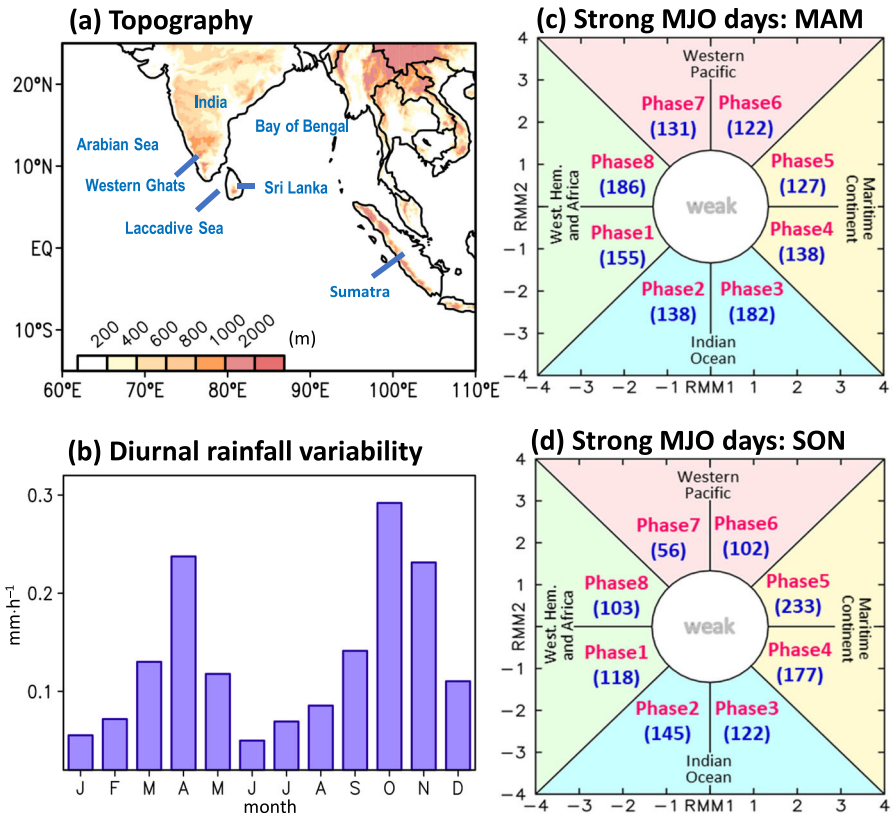

Fig. 1 | Background information for illustrating the study region and study events. a The regional map with topography (shaded). **b** The histogram with area-averaged diurnal rainfall variability (obtained from the standard deviation of hourly rainfall) over Sri Lanka for each month averaged from 2001 to 2020. **c** Phase defined by RMM1/RMM2, with the separation of strong MJO days for each MJO phase in spring during 2001–2020. **d** as in **c**, but for autumn.

recently demonstrated that the annual-averaged diurnal rainfall amplitude over Sri Lanka is enhanced during P2-to-P3 of MJO. They also found that the diurnal rainfall variation in Sri Lanka exhibits seasonal changes in the direction of its subsequent offshore propagation. This observed seasonality in diurnal rainfall patterns prompts the question of whether there are also seasonal differences in the MJO's modulation of diurnal rainfall characteristics, including amplitude and propagation, over Sri Lanka. Nonetheless, these documented studies mainly focused on the MJO's impact on the magnitude change of daily[17,20] or diurnal[31] rainfall in Sri Lanka. A notable knowledge gap exists in comprehending the effect of the MJO on the offshore propagation of diurnal rainfall in Sri Lanka.

Previous studies[9–11,16,22,24] investigating the MJO's impact on diurnal rainfall variation in different regions have primarily concentrated on either the summer season, characterized by active local diurnal convection, or the winter season, marked by active MJO convection. However, in the context of Sri Lanka, it was known that spring and autumn exhibit greater diurnal rainfall variability compared to winter and summer[31] (Fig. 1b and Supplementary Fig. 1). Therefore, this study specifically targets spring and autumn, hypothesizing that the seasonal differences in diurnal rainfall variability over Sri Lanka during spring and autumn might be attributed to the MJO activities in these two seasons. It was known that during spring and autumn, diurnal rainfall over Sri Lanka typically occurs in the afternoon, peaking around 5 pm local time (hereafter denoted as afternoon diurnal convection or ADC events). The ADC events then mainly propagated westward from inland Sri Lanka to nearby seas from 5 pm to early morning[31]. This westward propagation of diurnal rainfall during spring and autumn in Sri Lanka differs from the eastward propagation of summer diurnal rainfall seen in nearby South India[15] or the north-west to south-east movement of summer diurnal convective systems along the east coast of India[29]. This disparity in diurnal rainfall propagation directions implies that the findings of Prajwal et al.[15] or Mishra et al.[29] in explaining the MJO modulation of diurnal rainfall propagation over neighboring India may not be directly applicable to Sri Lanka. Building upon these insights, we aim to examine diurnal rainfall propagation over Sri Lanka and adjacent seas using the latest satellite precipitation data for each MJO phase, an aspect that has not been explored in prior research[17,20,31].

Sri Lanka experiences the highest frequency of ADC events in the Indian subcontinent region (Supplementary Fig. 2), highlighting the importance of examining the variations of ADC events over Sri Lanka under MJO's influence. Inspired by Huang et al.[31], who examined the MJO's influence on annual-averaged diurnal rainfall features over Sri Lanka, this study focuses on strong MJO days and conducts specific examinations on the frequency of ADC days during spring and autumn. By specifically focusing on these seasons and the ADC weather pattern in the analysis, we aim to answer two questions: (a) What are the differences in ADC characteristics (including frequency, amplitude, and propagation direction) during different MJO phases? (b) What underlying physical mechanisms can explain the features mentioned in question (a)? Addressing these questions will provide valuable insights into how the MJO modulates rainfall characteristics over Sri Lanka and enhance our overall understanding of this phenomenon.

Results

General rainfall characteristics

Before examining the specific ADC events, we investigated the general rainfall characteristics associated with strong MJO days (number of days for spring and autumn documented in Fig. 1c, d) to introduce the climatological background and the seasonal variations observed over Sri Lanka. Statistically, the rainfall evolution during a day consists of two components: the mean of 24-h rainfall (daily mean value) and the variation of diurnal rainfall anomalies (without the daily mean value). According to Huang et al.[31], diurnal rainfall anomalies and their variability (measured by Eq. (3) in Methods) are closely connected to the development of ADC events within a day. Thus, we conducted separate examinations for the MJO's modulation on daily mean rainfall and diurnal rainfall variability to clarify any potential differences between them.

Figure 2 reveals the detailed spatial distribution of daily mean rainfall over Sri Lanka (zoom-in on the left panel) and the associated distribution of

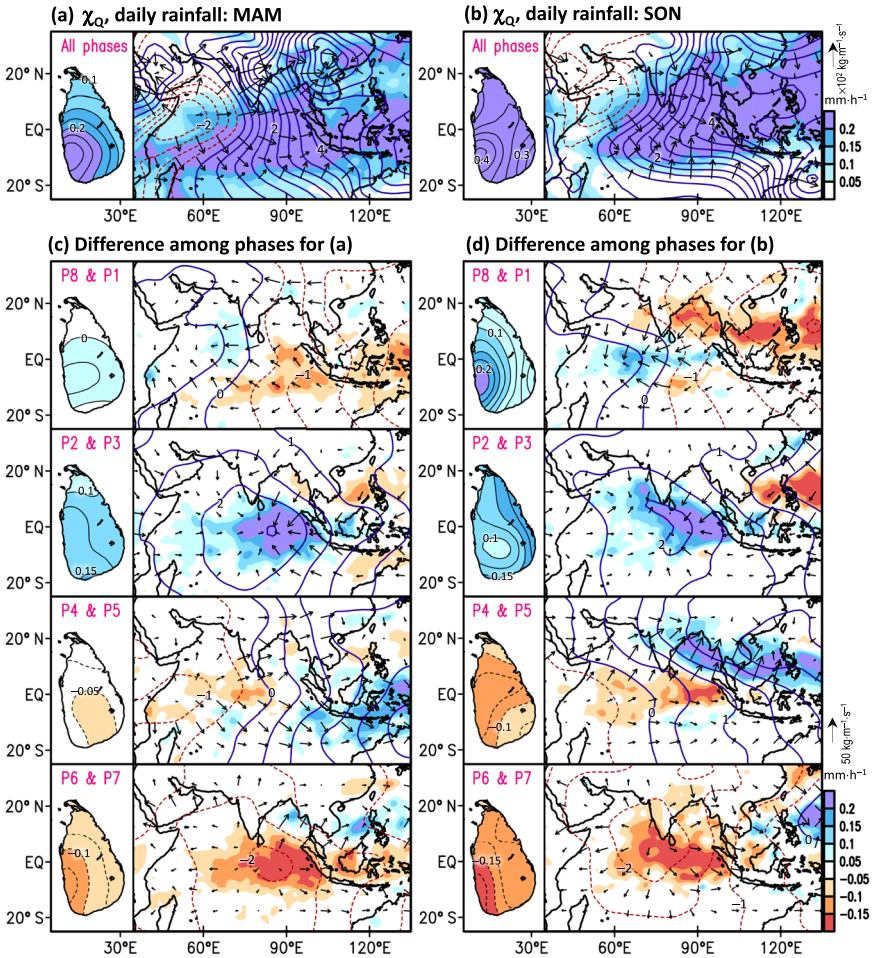

Fig. 2 | Climatological feature and MJO's modulation on the daily mean rainfall and moisture flux convergence. Contours over the larger domain represent the horizontal distribution of the composites of the potential function of vertically integrated moisture flux (denoted as χ_Q; positive and negative values indicate convergence and divergence, respectively; units: kg·s $^{-1}$) for strong MJO days in (**a**) spring and (**b**) autumn. The vectors and shaded areas represent the corresponding vertically integrated moisture flux vectors and daily mean rainfall, respectively. In **c** and **d**, the figures represent the difference between the composites at respective phase clusters (labeled) and the average of all eight MJO phases for spring and autumn, respectively. The left panel of each sub-figure provides a zoomed-in view of the rainfall distribution (shaded and contours) over Sri Lanka.

the potential function of moisture flux convergence/divergence across a larger domain (contour in the right panel). Climatologically (Fig. 2a, b), more moisture flux convergence is observed over Sri Lanka and its adjacent regions. The seasonal difference in moisture flux convergence leads to a larger daily mean rainfall over Sri Lanka in autumn (Fig. 2b) compared to spring (Fig. 2a). By examining the rainfall departure from Fig. 2a, b for each of the four MJO phase clusters (Fig. 2c, d), it becomes apparent that Sri Lanka experiences maximum (minimum) daily mean rainfall in P2-to-P3 (P6-to-P7), corresponding to larger-scale tropical moisture convergence (divergence) centered around the longitudinal region of Sri Lanka. These findings regarding the MJO's modulation on daily mean rainfall (see also Supplementary Fig. 3 for the area-averaged value) are consistent with the results of Jayawardena et al.[17], who examined similar features based on daily rainfall station observations over Sri Lanka. This similarity supports the robustness of our findings, which are inferred from modern satellite precipitation data.

Some noteworthy seasonal differences revealed in Fig. 2c, d warrant additional research attention. For example, over a larger domain, the rainfall band locations during P4-to-P5 shift from the south of the Maritime Continent in spring to the north of the Maritime Continent in autumn (see also Supplementary Fig. 4). A similar seasonal shift pattern is also noted by prior studies[6,32–34], indicating the seasonality of MJO's modulation on the regional rainfall distribution is a common feature seen in tropical islands. Additionally, the MJO's eastward propagation speed in the tropical regions in autumn (Fig. 2d) seems slower than in spring (Fig. 2c); this observation is confirmed by the Hovmöller diagram of outgoing longwave radiation and rainfall anomaly[8] averaged within 15°S-15°N (Supplementary Fig. 5a, b). This seasonal difference in the MJO's eastward propagation speed remains consistent even when the focused area shifts from the tropics (15°S-15°N) to the latitudinal zone of Sri Lanka (6°-9.5°N) (Supplementary Fig. 5c, d). However, within the narrower longitudinal span of Sri Lanka (80°-82°E), it becomes challenging to discern the MJO's influence on daily rainfall propagation, particularly inland. Notably, it might be possible to observe the MJO's modulation on the diurnal rainfall propagation, which is a more pronounced pattern over Sri Lanka during spring and autumn[31].

In addition to the daily mean rainfall, the diurnal rainfall variability over Sri Lanka also demonstrates a strong MJO modulation (Supplementary Fig. 6) and seasonal differences. The phase with the largest (smallest) diurnal rainfall variability appears in P2 (P5) in spring (Supplementary Fig. 6a). However, a different feature emerges for autumn, where the largest diurnal rainfall variability is observed in P1, one phase earlier than P2 (Supplementary Fig. 6b). The statistical analysis of the area-averaged diurnal cycle of hourly rainfall data in autumn over Sri Lanka between P1 and P2 (Supplementary Fig. 7) confirmed the significance of this phase difference, reaching at a 95% confidence level. In terms of the associated spatial patterns, Supplementary Fig. 6c, d also shows that Sri Lanka experiences maximum (minimum) diurnal rainfall variability during P2-to-P3 (P6-to-P7) in spring, whereas in autumn, this variability reaches a peak (bottom) during P8-to-P1 (P4-to-P5). Moreover, the magnitude difference between the maximum and minimum phase of diurnal rainfall variability is more pronounced in autumn than in spring, particularly over western Sri Lanka.

A comparison between Supplementary Fig. 3a, b with Supplementary Fig. 6a, b further highlights the differences in the MJO's modulation on the daily mean rainfall and the diurnal rainfall variability over Sri Lanka. The daily mean rainfall peaks in P2 for both spring and autumn, while the diurnal rainfall variability peaks in P2 for spring but in P1 for autumn.

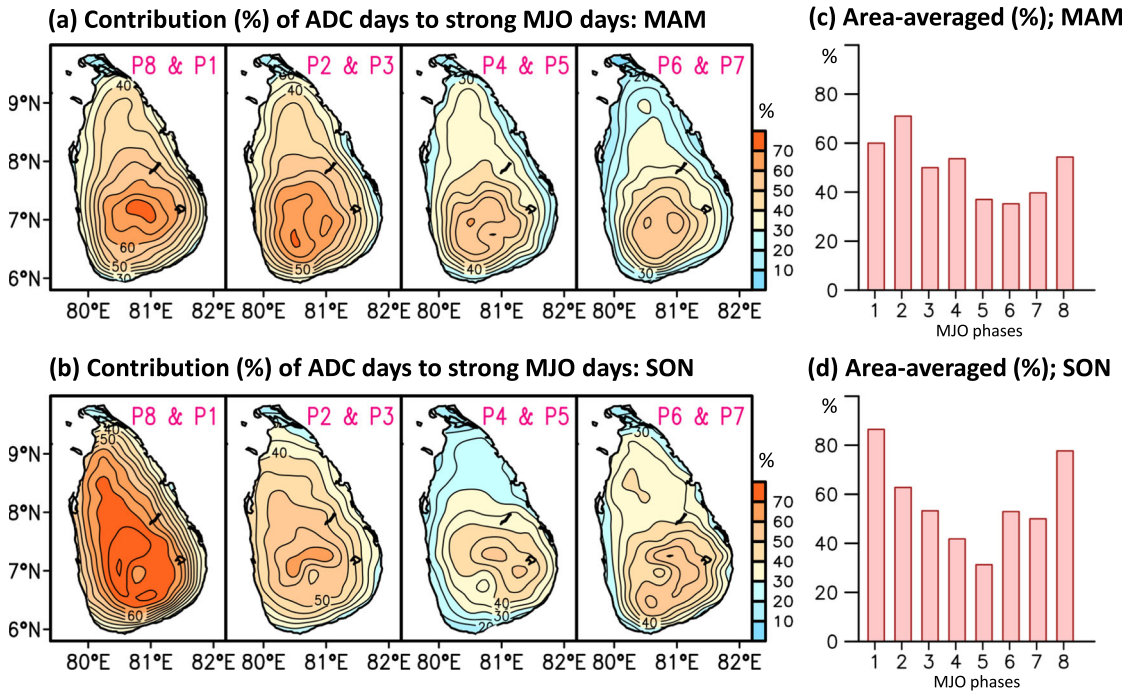

Fig. 3 | Examinations on the occurrence frequency of ADC events. a The chance of occurrence frequency of ADC events (Eq. (1) in Methods) for each grid box in the different phases of MJO averaged during the spring of 2001–2020. **c** The area-averaged percentage contribution value related to **a** for each MJO phase. **b** and **d** as in **a** and **c**, respectively, but for the autumn.

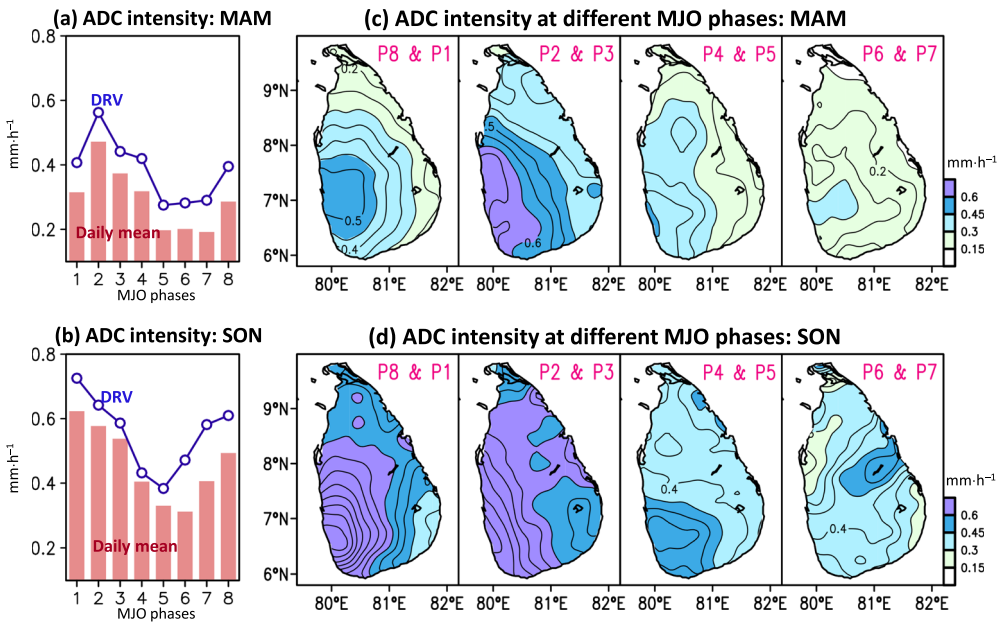

Fig. 4 | Examinations on the intensity of ADC events. a The area-averaged rainfall intensity (daily mean; pink bar) and diurnal rainfall variability (DRV; blue line) estimated from ADC days over Sri Lanka during strong MJO modulations over the spring of 2001–2020. **c** As in **a**, but for the spatial distribution of different MJO clusters. **b** and **d** as in **a** and **c**, respectively, but for the autumn.

Considering that the larger diurnal rainfall variability is the main feature of ADC events over Sri Lanka[22], it is possible that the MJO's modulation on ADC events also exhibits differences in the peak phase similar to what was observed in Supplementary Fig. 6a, b. To further clarify this inference, we sequentially examined the occurrence frequency, intensity, and propagation of ADC events during the strong MJO modulation in the next subsection. Notably, the number of strong MJO days varies across phases and seasons (Fig. 1c, d). Therefore, our analysis of ADC event frequency (Fig. 3) primarily focuses on the occurrence percentage of ADC days relative to strong MJO days (Eq. (1) in Methods) for each MJO phase, ensuring a more logical and meaningful comparison.

Impact of MJO on ADC events

Figure 3a, b shows the spatial distribution of the occurrence percentage of ADC days relative to the strong MJO days under four MJO phase clusters during spring (autumn). Visually, in both spring and autumn, a higher

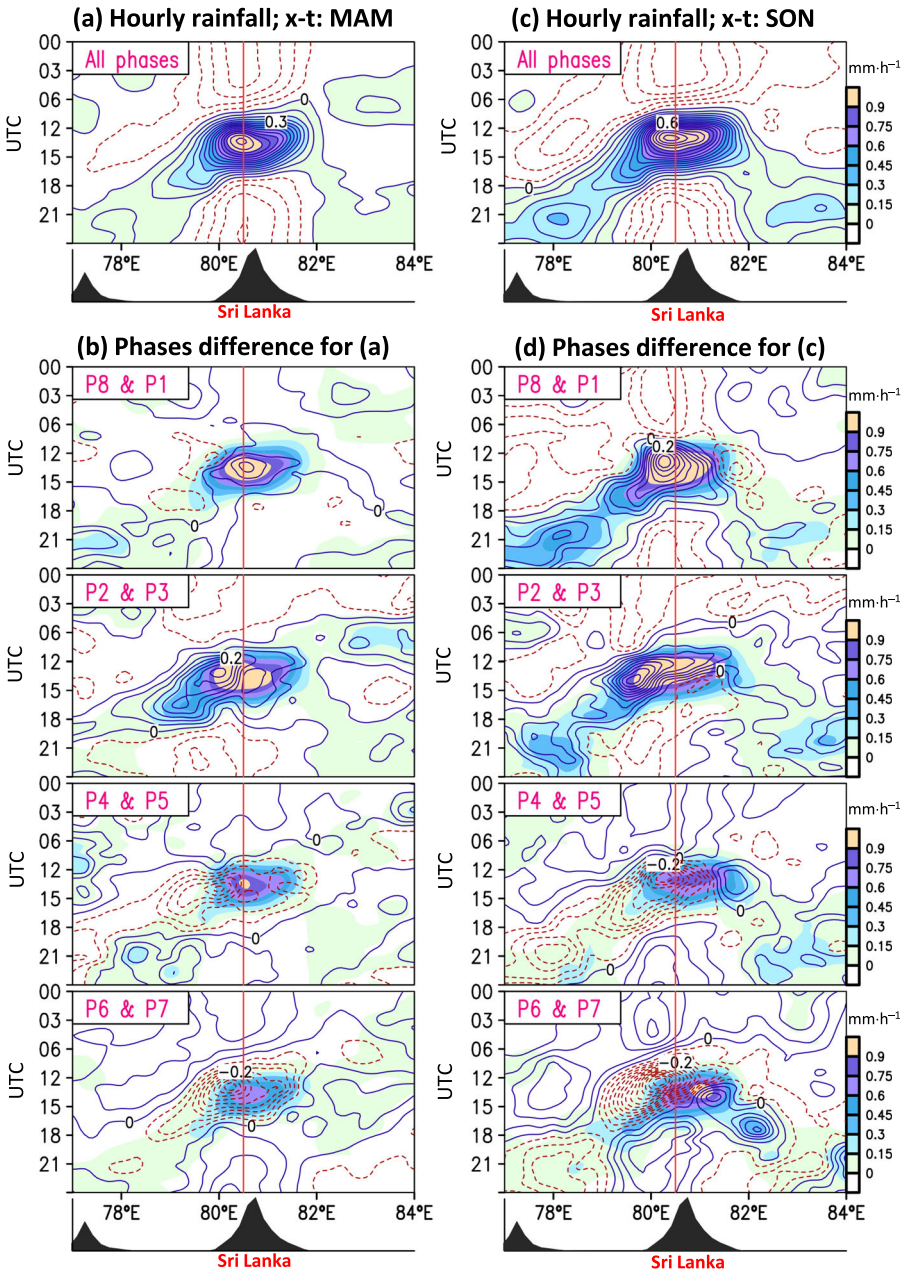

Fig. 5 | Examinations on the diurnal propagation of ADC events. a The longitude-time diagram of hourly rainfall anomalies (daily mean removed) averaged over the latitudinal zone (6°-9.5°N) of Sri Lanka for the composites from ADC events under strong MJO modulation during the spring of 2001–2020 (shaded and contoured). **b** is related to **a**, but for the composites of ADC days in different MJO phases (shaded area) superimposed with the composites minus (**a**) (contoured). **c** and **d** as in **a** and **b**, respectively, but for the autumn. The bottom panel includes the topography profile averaged over 6°-9.5°N. The red solid lines represent the longitudinal locations of maximum rainfall over Sri Lanka, identified from **a** and **b**. These red lines are added in **c** and **d** as reference points for comparing phase differences.

probability of ADC events occurs around the mountainous region of Sri Lanka for all MJO clusters. However, the maximum and minimum phase for MJO's modulation on the percentage contribution of ADC events to the strong MJO days in autumn (Fig. 3b) differs from spring (Fig. 3a). In autumn (spring), the percentage contribution is higher in P8-to-P1 (P2-to-P3) and lower in P4-to-P5 (P6-to-P7). This slight difference in the MJO's modulation of ADC events between spring and autumn contributes to the observed seasonal variations.

The related area-averaged value of ADC's occurrence percentage for each of the eight MJO phases is provided in Fig. 3c, d for spring (autumn). A seasonal difference is observed between Fig. 3c and d, where the maximum (minimum) phase occurs in P2 (P6) for spring and in P1 (P5) for autumn. Additionally, the magnitude difference between the maximum and minimum values among the eight MJO phases is greater in autumn (Fig. 3d) than in spring (Fig. 3c). This indicates that MJO's impact on the occurrence frequency of ADC events is more pronounced in autumn than in spring. To examine whether the MJO's impact on the ADC's intensity (Eq. (2) in Methods) also shows seasonal differences, we constructed the related area-averaged rainfall intensity of ADC events for the eight MJO phases. Results also show that ADC events are more intense during autumn (Fig. 4b) than in spring (Fig. 4a).

Additionally, we noted from Fig. 4a, b (bars) that the largest magnitude of rainfall intensity for ADC events occurs in P2 (P1) for spring (autumn), while the smaller rainfall intensity of ADC events appears in P5 for both spring and autumn. These phase changes in the intensity of ADC events (Fig. 4a, b) not only roughly correspond to the phase change in ADC's occurrence percentage (Fig. 3c, d) but also to the phase change in diurnal rainfall variability (see line graph in Fig. 4a, b) under the MJO's modulation. In terms of spatial patterns, unlike the occurrence frequency (Fig. 3a, b), the rainfall intensity distribution of ADC events (Fig. 4c, d) is asymmetric, with higher values observed over the western side of the central mountain range (i.e., the windward side of low-level westerly wind[22]) compared to the eastern side of the central mountain range for most MJO phases in both spring and autumn. This spatial pattern also corresponds to the distribution of diurnal rainfall variability (Supplementary Fig. 6c, d), confirming the importance of ADC events in contributing to the diurnal rainfall variation over Sri Lanka.

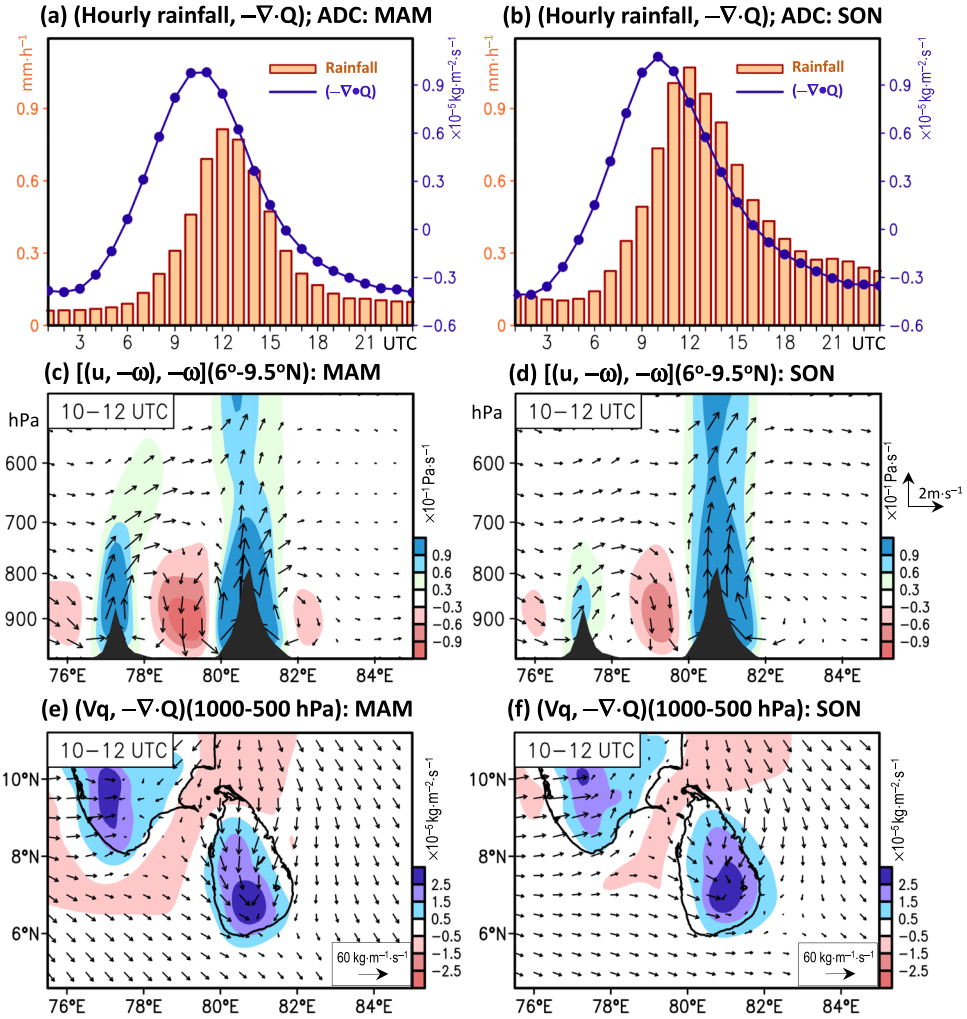

Fig. 6 | Examinations on the maintenance mechanisms of ADC formation over Sri Lanka. This figure is constructed from ADC events under strong MJO modulation during (**a**) spring and (**b**) autumn of 2001–2020. **a** The composites of hourly rainfall (bar) and moisture flux convergence vertically integrated between 1000 and 500 hPa (line) in spring. **c** The composites of east-west vertical circulation [denoted as $(u, -\omega)$; vectors] superimposed with vertical motion $(-\omega)$ along the latitudinal zone (6°-9.5°N) during 10–12 UTC, with daily mean removed, in spring. **e** The composites of vertically integrated moisture flux convergence [denoted as $-\nabla\cdot Q$; shaded] superimposed with vertically integrated moisture flux vectors during 10–12 UTC, with daily mean removed, in spring. **b**, **d**, and **f** as in **a**, **c**, and **e**, respectively, but for the autumn.

The MJO's impact on the ADC events can also be seen in the diurnal rainfall propagation. Figure 5a, c shows the Hovmöller diagram of hourly rainfall evolution departure from the daily mean values and composited from all ADC events over Sri Lanka during spring (autumn). The hourly evolution of the average of all ADC events (Fig. 5a) shows a maximum of rainfall at 12 UTC (5:30 pm), followed by predominant westward propagation toward the nearby Laccadive Sea around 18 UTC (11:30 pm). This propagating feature for ADC events is similar to those documented by Huang et al.[31] for all spring days, implying that the ADC events primarily govern the westward propagation of the diurnal rainfall feature observed in spring. By separating the features into different MJO phase clusters, we further noted that during P2-to-P3 (Fig. 5b), there were not only more enhanced ADC events occurred over the land area of Sri Lanka but also a relatively apparent westward propagation feature, when compared to other MJO phases in spring.

Regarding autumn, the results shown in Fig. 5c, d indicated the following propagation features: (1) for climatology, the westward propagation is more apparent than the eastward propagation during a day as observed from the composites of all ADC events (Fig. 5c), and (2) for the MJO modulation, a more pronounced westward propagation compared to the eastward propagation observed in P8-to-P1 and P2-to-P3 than in other MJO phases (Fig. 5d). Although we observed similar propagation characteristics in both spring (Fig. 5a, b) and autumn (Fig. 5c, d), there are still some differences between them. For the climatology, the eastward propagation is primarily evident in autumn (Fig. 5c) and to a lesser degree in spring (Fig. 5a). The significant testing results shown in Supplementary Fig. 8a, c supports this observation. Possible causes for this seasonal difference in the climatology of diurnal rainfall propagation between spring and autumn have been examined by Huang et al.[31], and they attributed this to the seasonal difference in the interactions between atmospheric circulation and local topography.

As for the MJO's modulation, we observed a seasonal difference in the occurrence phase for the enhanced westward diurnal rainfall propagation over Sri Lanka. The enhanced westward propagation mainly occurred in P2-to-P3 during spring (Fig. 5b and Supplementary Fig. 8b). In contrast, the most apparent enhanced westward propagation occurred in P8-to-P1 during autumn (Fig. 5d and Supplementary Fig. 8d). This observation aligns with the previously noted feature that the peak rainfall intensity of ADC events in autumn (P1) occurs one phase earlier than in spring (P2). Additionally, it is worth noting that in autumn, there is enhanced eastward propagation from eastern Sri Lanka to nearby sea occurring in P4-to-P5 and P6-to-P7 (Supplementary Fig. 9a).

Physical maintenance mechanisms of ADC events: climatology

Next, prior to examining the physical maintenance mechanisms related to MJO's modulation, we analyzed the atmospheric thermodynamic conditions crucial to the climatological characteristics of ADC events. The time series analysis presented in Fig. 6a, b is derived from the composites of area-averaged hourly rainfall and moisture flux convergence for all ADC events over Sri Lanka during spring (autumn). Our analysis revealed that the ADC events in Sri Lanka during both spring and autumn typically occur on days with a maximum moisture flux convergence occurring around 10–11 UTC, followed by an hourly rainfall maximum appearing around 12 UTC. The

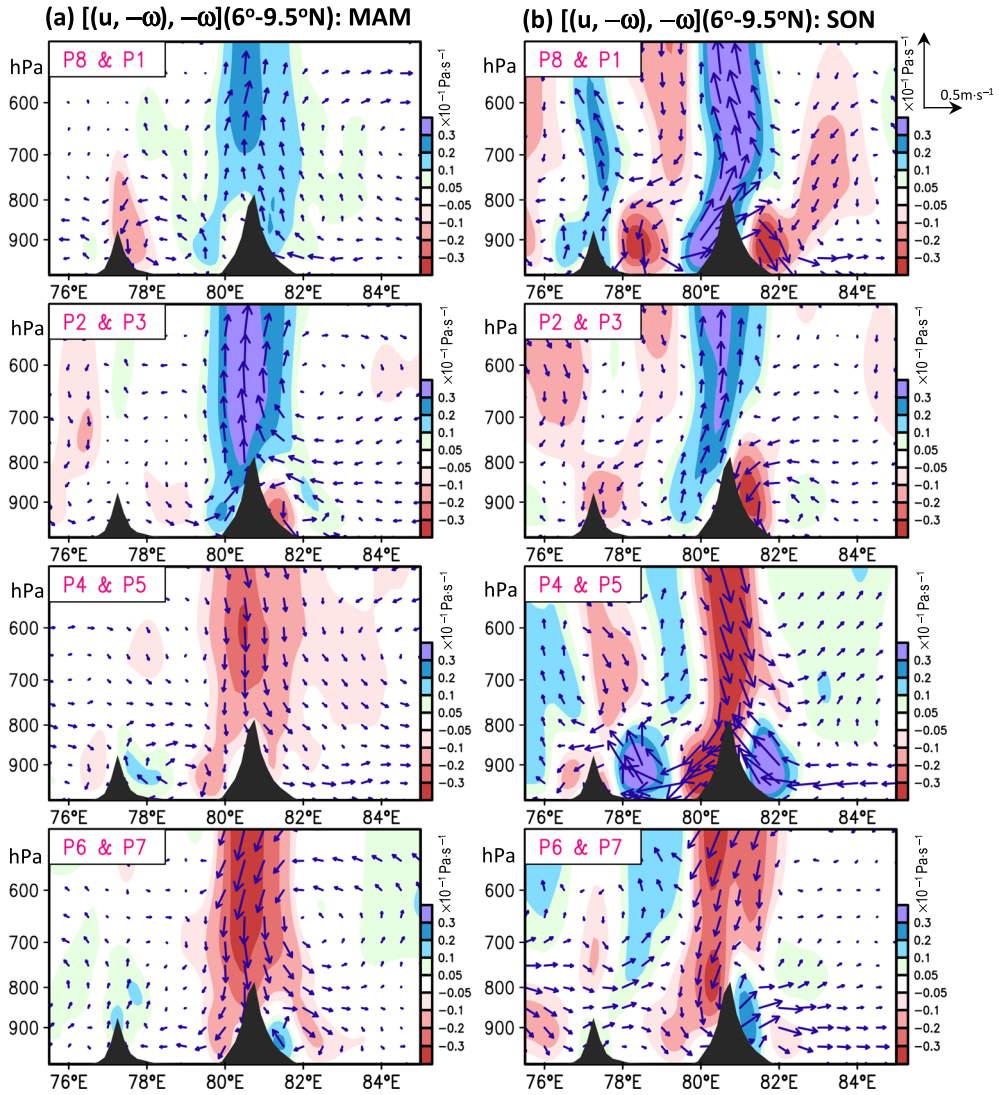

Fig. 7 | MJO's modulation on the east-west circulation changes along the latitudinal zone (6°-9.5°N). The figure is constructed from the difference between the MJO phase clusters and the average of all eight MJO phases. From top to bottom are the phase clusters of P8-to-P1, P2-to-P3, P4-to-P5, and P6-to-P7, respectively. The wind vectors illustrate the changes in the zonal wind (u) and vertical motion ($-\omega$) for the composites from ADC events under strong MJO modulation during (**a**) spring and (**b**) autumn of 2001–2020. The shaded area represents the vertical motion changes. These variables are averaged during 10–12 UTC, which is the time period from maximum water vapor support (10–11 UTC) to maximum rainfall (12 UTC), with the daily mean removed.

time period of 10–12 UTC, which is the time from the maximum water vapor flux support to the maximum hourly rainfall, is selected for further examinations herein. Upon examination of the vertical cross-section of east-west anomalies (daily mean removed) circulation averaged during 10–12 UTC over Sri Lanka (Fig. 6c, d), we observed that the afternoon convections with active upward motion are induced by the onshore breeze during the daytime. The upward motion is more active in autumn than in spring over Sri Lanka, partly explaining the larger amplitude of diurnal rainfall variation in autumn than in spring.

The relationship between vertical motions in the regions of 76°-78°E (around South India) and 80°-82°E (around Sri Lanka), as depicted in Fig. 6c, d, is influenced by a combination of factors, including topography and locally induced east-west circulation driven by the land-sea breeze[31]. For spring, in comparison to autumn, there is a more pronounced upward motion in the 76°-78°E area, potentially leading to a stronger downward motion in the 78°-80°E region at 10–12 UTC. Consequently, this pattern, coupled with a stronger low-level divergence over the Laccadive Sea, further induces stronger sea breezes over western Sri Lanka in spring than in autumn. As a result, the upward motion over western Sri Lanka is more prominent during spring than in autumn, explaining the slight westward shift in the distribution of maximum upward motion over Sri Lanka in spring as compared to autumn.

The abovementioned feature observed in Fig. 6c, d is better illustrated in Fig. 6e, f, which shows the horizontal distribution of vertically-integrated moisture flux convergence during 10–12 UTC. These findings confirm that the changes in regional moisture and wind circulation substantially impact the formation of ADC events in Sri Lanka during spring and autumn. Huang et al.[31] also suggested similar mechanisms for all general days rather than the strong MJO days and ADC events. Given that the MJO has the potential to influence atmospheric thermodynamic conditions[35], it is likely that the MJO can also modulate the characteristics of the ADCs in spring and autumn through the associated changes in the related atmospheric thermodynamic conditions.

Physical maintenance mechanisms of ADC events: MJO's impact

To clarify the above inference, we constructed the phase differences for the maintenance mechanisms that are important for ADC formation. Figure 7 displays the vertical cross-section of atmospheric circulation for the selected phases, with the average of all eight MJO phases subtracted for spring

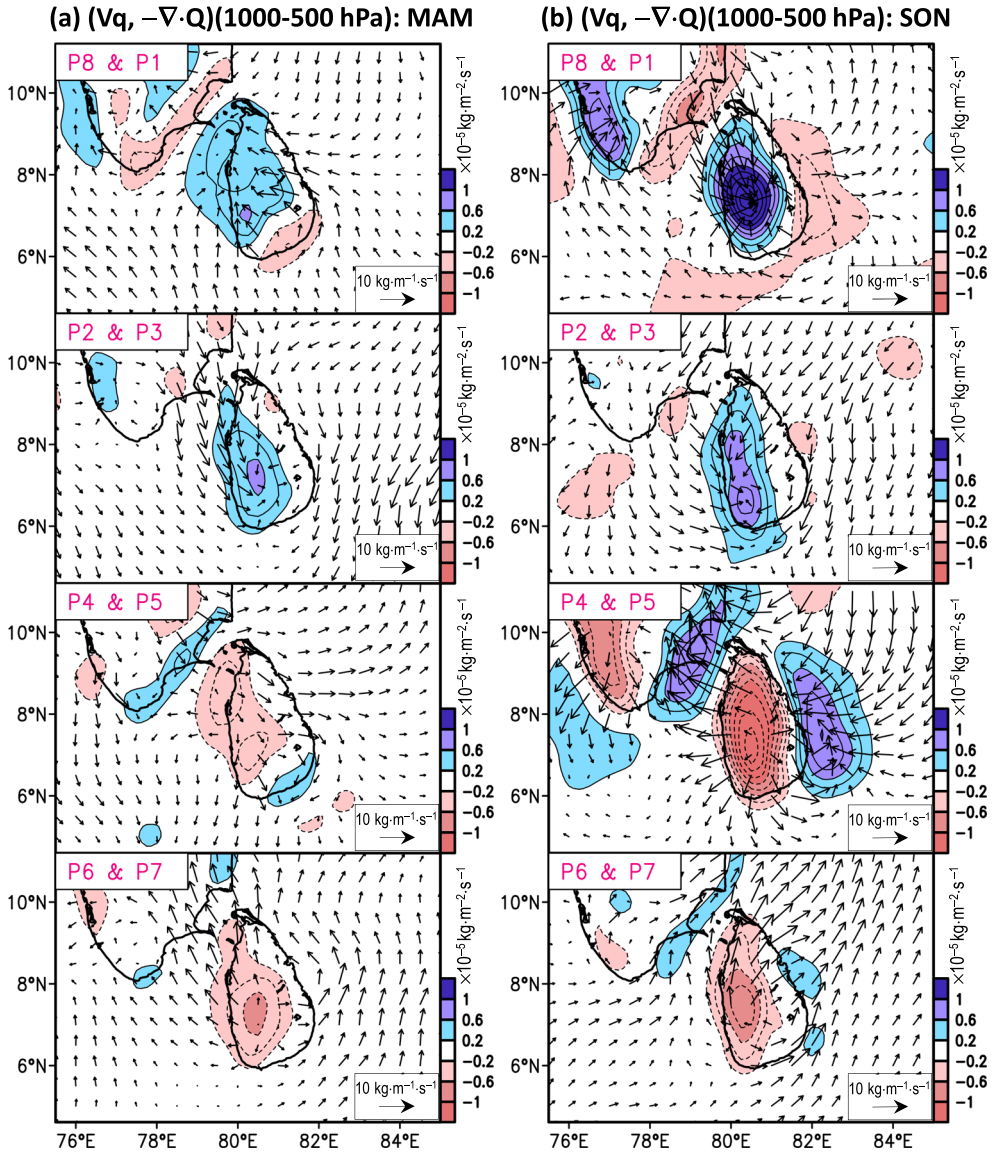

Fig. 8 | MJO's modulation on the moisture flux changes. Similar to Fig. 7, but for horizontal distribution of the difference between MJO phase clusters and the average of all eight MJO phases for vertically integrated (between 1000 and 500 hPa) moisture flux convergence [denoted as (−∇·*Q*); shaded], superimposed with vertically integrated moisture flux vectors under strong MJO modulations during (**a**) spring and (**b**) autumn of 2001–2020. These variables are averaged during 10–12 UTC, with the daily mean removed.

(Fig. 7a) and autumn (Fig. 7b). It was observed that the afternoon upward motion induced by the low-level wind convergence averaged during 10–12 UTC was enhanced in the MJO phase clusters of P8-to-P1 and P2-to-P3. Conversely, although with varying magnitudes, a suppressed pattern was revealed in the MJO phase clusters of P4-to-P5 and P6-to-P7 in both seasons. This feature is more consistent between the vertical level of 800 hPa to 500 hPa.

For the seasonal difference, it is also revealed that the maximum upward motion over Sri Lanka occurred during the P2-to-P3 cluster in spring and the P8-to-P1 cluster in autumn (Fig. 7). Within the atmospheric layer spanning from the surface to 800 hPa, the interplay between topography and land-sea circulation plays a pivotal role in shaping the distribution of vertical motion[31]. Generally, during spring (autumn), the enhanced upward motion in the P2-to-P3 (P8-to-P1) cluster is predominantly observed on the windward side, which corresponds to western Sri Lanka. In contrast, the leeward side, corresponding to eastern Sri Lanka, exhibits enhanced downward motion. These features (Fig. 7) align well with the typical characteristics of local thunderstorm formation, where at low levels, upward motion occurs on one side and downdraft on the other side of the system coupled with an active upward motion in the middle levels[36]. A converse pattern is revealed in the MJO phase clusters of P6-to-P7 (P4-to-P5) in spring (autumn), with enhanced west-east distribution of downward-upward motion in Sri Lanka at the levels below 800 hPa, which coupled with the downward motion above 800 hPa over Sri Lanka, implying the local thunderstorm has been suppressed. Despite the magnitude differences among phases, the above features are valid for both spring (Fig. 7a) and autumn (Fig. 7b). However, these upward/downward motion features are more pronounced during autumn than in spring.

Additionally, when comparing Fig. 5d with Fig. 7b, as depicted in Supplementary Fig. 9, it becomes further evident that the MJO phases with enhanced upward motion over western (eastern) Sri Lanka are the phases with enhanced westward (eastward) propagation of diurnal rainfall features. To further investigate whether the local moisture flux convergence (i.e., a crucial mechanism for maintaining the formation of the ADC events) exhibited similar phase discrepancies, we constructed Fig. 8. This figure displays the spatial distribution of the phase differences (after subtracting

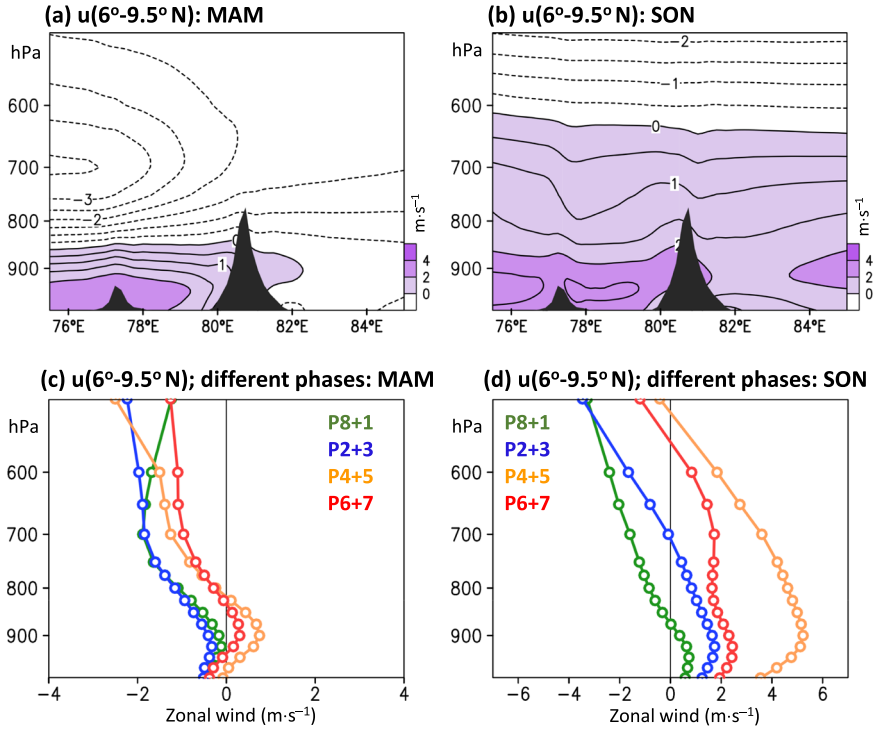

Fig. 9 | MJO's modulation on the zonal wind circulation changes along the latitudinal zone (6°-9.5°N). a and **b** are the composites from ADC events under strong MJO modulation in spring and autumn, respectively. **c** and **d** are related to **a** and **b**, respectively, but for the area-averaged zonal wind (u) over Sri Lanka estimated from different phase clusters. The color legends in the right and left top panels for **c** and **d** represent the different MJO phase clusters.

the average of all eight MJO phases) in the local moisture flux convergence on days with strong MJO modulation during the spring (Fig. 8a) and autumn (Fig. 8b) spanning the period from 2001 to 2020.

Several key features for Fig. 8 are summarized as follows: (1) the larger phase differences of moisture flux convergence are primarily observed over western Sri Lanka, which helps explain the location differences observed in the maximum intensity of ADC composites, as shown in Figs. 4c, d, (2) the magnitude difference among different phases is more pronounced in autumn compared to spring, which accounts for the seasonal changes in diurnal rainfall amplitude difference among various MJO phases as seen in Fig. 5b, d and (3) the largest enhancement of moisture flux convergence observed during P2-to-P3 cluster in spring and in P8-to-P1 cluster in autumn, which explains the seasonal differences in the MJO's modulation on the occurrence (Fig. 3) and intensity (Fig. 4) of ADC events over Sri Lanka. Also note that western Sri Lanka, which is the windward side of the prevailing low-level westerly wind (Fig. 2a, b), experiences larger changes in moisture flux convergence under different MJO phases (Fig. 8). These findings provide valuable insights into how the local thermodynamic conditions (including the interaction between topography and land-sea breezes) associated with the propagation of the MJO have changed. Consequently, these changes have led to variations in the occurrence frequency and intensity of ADC events in Sri Lanka.

In Fig. 8b, a prominent convergence (divergence) center emerges over Sri Lanka during P8-to-P1 (P4-to-P5) while diverging (converging) in the surrounding ocean that near South India and the eastern side of Sri Lanka. This implies that the climatological afternoon moisture convergence pattern (Fig. 6f) is strengthened in P8-to-P1 but weakened in P4-to-P5 under the influence of the MJO. This short-wave-train like pattern is predominantly observed in autumn (Fig. 8b) and less prominent in spring (Fig. 8a), signifying a seasonal diversity of the MJO's modulation of magnitude changes in the regional vertically-integrated moisture flux. This seasonal difference explains why the MJO's modulation on the ADC's amplitude is more pronounced in autumn (Fig. 4b) than in spring (Fig. 4a). Similarly, Lu et al.[37] have also highlighted the significance of seasonal changes in the vertically-integrated moisture flux caused by diurnal winds in explaining seasonal differences in the diurnal rainfall cycle under the MJO's modulation, with a focus on the Maritime Continent.

Finally, the potential factors contributing to the enhanced or suppressed westward propagation of ADC events seen in Fig. 5 are examined. Huang et al.[31] demonstrated that the mid-to-upper-level easterly winds present during spring and autumn are crucial in driving the westward propagation of diurnal rainfall convection over Sri Lanka. Expanding upon the work of Huang et al.[31], we analyzed the area-averaged zonal wind over Sri Lanka for the composites of ADC events and focused on the MJO's modulation. Figure 9 presents the vertical distribution of zonal wind changes averaged over the latitudinal region of Sri Lanka for the composites of ADC events during strong MJO days in spring (Fig. 9a) and autumn (Fig. 9b). In both seasons, the zonal wind shows a reverse wind direction from westerly wind in the lower levels to the easterly wind in the upper levels over the region of 78°-80°E that covers the western coast of Sri Lanka and Laccadive Sea. The change in wind direction occurred at a higher level in autumn than in spring. Specifically, the transition occurred around 850 hPa in spring and 600 hPa in autumn. These patterns align with the observations made by Huang et al.[31] for the composites of climatological seasonal features.

For the MJO's modulation, we observed that in spring, the mid-to-upper-level easterly wind appeared in all four MJO phase clusters (Fig. 9c). However, the wind speed between 850 hPa to 600 hPa is stronger in P8-to-P1 and P2-to-P3 than in P4-to-P5 and P6-to-P7 clusters. In autumn, a similar enhancement of upper-level easterly wind appeared between 700 hPa to 500 hPa in P8-to-P1 and P2-to-P3 than in P4-to-P5 and P6-to-P7 clusters (Fig. 9d). As inferred from these observations, when a deeper ADC event occurred in P2-to-P3 during spring (as in Fig. 9a) and in P8-to-P1 during autumn (as in Fig. 9b), it can be modulated by the enhanced mid-to-upper level easterly wind to propagate further westward. This explains the diurnal propagation features seen in Fig. 5. However, it is important to note that for spring (Fig. 9c), even though the P8-to-P1 cluster has a magnitude of easterly wind between 800 hPa and 600 hPa, similar to the P2-to-P3 cluster, the westward propagation of ADC event in P8-to-P1 cluster is not as pronounced as those observed in P2-to-P3 cluster (Fig. 5b). This could be attributed to the weaker intensity of ADC events over Sri Lanka during P8-to-P1 compared to P2-to-P3 in spring (Fig. 4a).

Discussion

In view of earlier literatures[17,20,31], a knowledge gap exists in comprehending how the MJO influences the ADC's characteristics (particularly the offshore rainfall propagation) over Sri Lanka. This study thoroughly examines this issue and explains the potential underlying physical mechanisms. As summarized in the schematic diagram (Fig. 10), low-level westerly winds and sea breeze interacting with topography (Step 1) can induce moisture flux convergence accompanied by upward motion (Step 2), which leads to ADC's formation with rainfall (Step 3), over Sri Lanka. This deep convection is subsequently modulated by the prevailing upper-level easterly winds to lead more westward offshore propagation from western Sri Lanka to nearby seas (Step 4). These ADC's maintenance mechanisms reach their maximum (minimum) values during MJO phases P2-to-P3 (P6-to-P7) and P8-to-P1 (P4-to-P5) in spring and autumn, respectively. As a result, enhanced (suppressed) ADC's occurrence frequency percentage, rainfall intensity, and westward propagation have been observed during MJO's active (inactive) phases over Sri Lanka. These findings hold significant implications for the regional community. For example, the observed link between changes in ADC characteristics and MJO phases could be leveraged to improve the local rainfall forecasting capabilities. More accurate rainfall forecasts, in turn, play an integral role in flood mitigation, improving agricultural productivity and contributing to the broader realm of sustainable development initiatives in the region.

Notably, in addition to the mechanisms outlined in Fig. 10, there might be some additional factors important to the ADC's formation. As inferred from other studies[15,29] focusing on various tropical regions, it is conceivable that the MJO's impact on regional rainfall could be influenced by changes in convective available potential energy (CAPE) and relative humidity. These potential mechanisms merit further detailed analyses specific to Sri Lanka. Moreover, the findings of the present study, based on observational data, can be further complemented by future studies using model simulations[38,39] to clarify the details of the topographic effect on ADC events under MJO's modulation. Furthermore, it is known that MJO-induced extreme rainfall might change in response to global warming[21]; thus, exploring how ADC's characteristics may change in response to global warming[40,41] also deserves further research attention for the region over Sri Lanka.

Methods

Rainfall data and reanalysis data

The rainfall data used for the definition of ADC events over Sri Lanka are extracted from version 6 (V06B) final run of the Integrated Multi-satellitE Retrievals for Global Precipitation Measurement (IMERG) product, which is a dataset with 30-minute temporal resolution and $0.1° \times 0.1°$ spatial resolution[42]. Sub-daily IMERG data have already been successfully validated using the local rain gauges over Sri Lanka, and for further information and validation results, please refer to Huang et al.[31]. Additionally, for the examination of the related physical mechanisms, we extracted the atmospheric thermodynamic variables (including wind and specific humidity) from the latest 5th generation of the European Centre for Medium-range Weather Forecast reanalysis data (ERA5)[43]. The spring and autumn seasons were defined as periods from March to May (MAM) and September to November (SON), respectively. The analysis focuses on the overlapping common period of available data from IMERG and ERA5, which is from 2001 to 2020.

Definition of MJO phases

The Real-time Multivariate MJO Index (RMM1 and RMM2), developed by Wheeler and Hendon[44], is extensively employed worldwide to identify and categorize MJO events into 8 distinct phases[13,45–47]. For this study, we obtained the RMM indexes from the Australian Bureau of Meteorology, and the data can be accessed at http://www.bom.gov.au/climate/mjo/. A day is considered to have a strong (weak) MJO modulation when the amplitude of the RMM index ($=\sqrt{RMM1^2 + RMM2^2}$) is greater than 1 (less than 1). This study focused only on days with strong MJO modulation from 2001 to 2020. The general rainfall characteristics subsection in the Results includes a detailed analysis of the number of strong MJO days over the given period for spring (Fig. 1c) and autumn (Fig. 1d). Colors have been added in Fig. 1c, d, to help represent the MJO's propagation into different locations (i.e., P8-to-P1 in the western hemisphere and Africa, P2-to-P3 in the Indian Ocean, P4-to-P5 in the Maritime Continent, and P6-to-P7 in the western Pacific). This grouping method, which is commonly used in earlier studies[45–47] to explore features related to MJO propagation, is adopted to examine MJO composites.

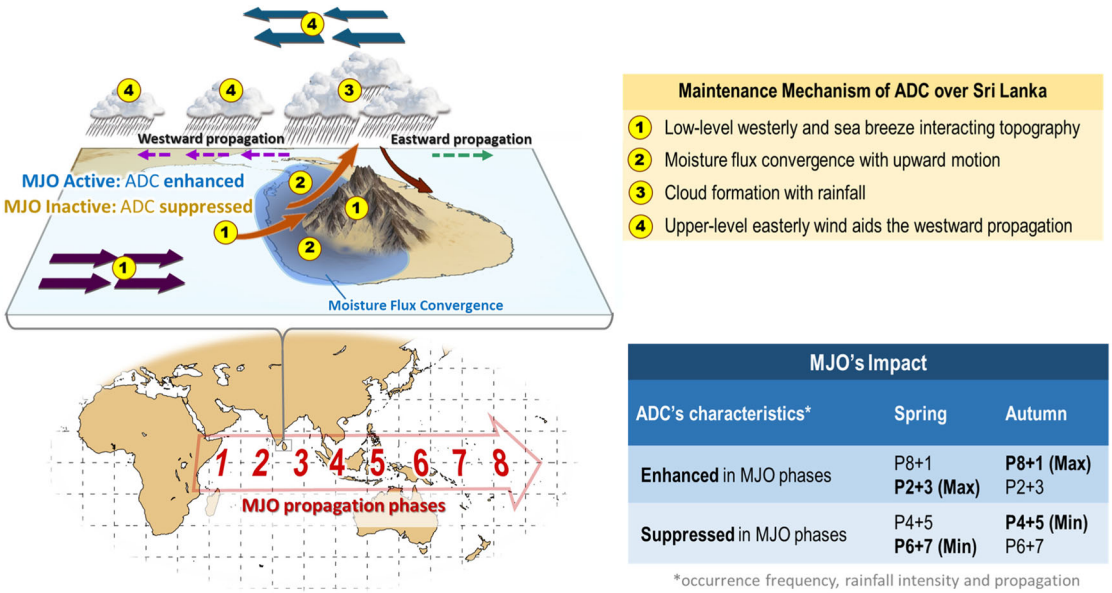

MJO's Impact		
ADC's characteristics*	Spring	Autumn
Enhanced in MJO phases	P8+1 **P2+3 (Max)**	**P8+1 (Max)** P2+3
Suppressed in MJO phases	P4+5 **P6+7 (Min)**	**P4+5 (Min)** P6+7

*occurrence frequency, rainfall intensity and propagation

Fig. 10 | Schematic diagram summarizing the MJO's impact on ADC's characteristics. The top left panel illustrates the formation of ADC over Sri Lanka following four main steps, which are detailed in the top right panel. The bottom left panel roughly illustrates the general locations of the eight MJO phases and their propagation direction, with the bottom right panel documenting the ADC's characteristics changes (including the relative changes in occurrence frequency, rainfall intensity, and westward propagation) between spring and autumn under different MJO phase modulations.

Definition of ADC events

In this study, a rainy day is defined as a day when more than one-third of the grid box over the domain of Sri Lanka has a daily accumulation of rainfall greater than 0.1 mm. The selection of 0.1 mm as criteria for identifying rainy days has been widely adopted by earlier studies using IMERG data[48–50]. After identifying a rainy day, the occurrence of an ADC event for each grid box is defined based on the following criteria: (a) The accumulated rainfall between 01:00 and 11:00 local time should be less than 20% of the total daily rainfall, (b) The accumulated rainfall between 12:00 and 22:00 local time should exceed 70% of the total daily rainfall, and (c) The rainy pattern should remain unaffected by other non-local weather patterns, such as tropical cyclones. A day on which one-third of the grid box over the domain of Sri Lanka is identified as ADC is further referred to as an ADC day. Similar methods for identifying ADC events over an island have been applied by many studies[51–53].

The total number of ADC days during the analyzed period is referred to as ADC frequency. Supplementary Fig. 2 depicts the spatial distribution of the total accumulated number of ADC frequency (for each grid point) for strong MJO days during the spring and autumn of 2001–2020. Overall, during both seasons, the inland area exhibits a higher number of ADC days than the coastal area, with the largest number of ADC events (>500 days) occurring over the mountain region in southern Sri Lanka. In this study, the percentage occurrence of ADC days relative to strong MJO days for each MJO phase is calculated using Eq. (1), while the magnitude of ADC intensity is calculated using Eq. (2):

$$\text{Percentage occurrence of ADC days} = \frac{\text{Accumulated number of ADC days}}{\text{Total number of strong MJO days}}, \quad (1)$$

$$\text{ADC intensity} = \frac{\text{Accumulated daily rainfall amount for all ADC events}}{\text{Total number of ADC days}}, \quad (2)$$

As evident in our composite of ADC events (Fig. 6a, b), the daily accumulation of IMERG rainfall for ADC events is approximately 6.3 mm·day^{-1} for spring and 10.0 mm·day^{-1} for autumn. These values fall within the range of moderate rain (ranging from 5 to 20 mm·day^{-1}) as opposed to light rain (ranging from 0.1 to 5 mm·day^{-1})[54].

Diurnal rainfall variability

The diurnal rainfall variability[41,55] was calculated from the standard deviation of 24-hour rainfall for the selected samples (e.g., strong MJO days or total days) using Eq. (3):

$$\text{Diurnal rainfall variability} = \sqrt{\frac{\sum \left(\mathrm{R_i} - \bar{\mathrm{R}}\right)^2}{\mathrm{N}}}, \quad (3)$$

where R_i, $\bar{R}$ and N represents the hourly rainfall for each sample, the daily mean of the hourly rainfall, and the total number of samples, respectively. Generally, larger (smaller) values of diurnal rainfall variability correspond to higher (lower) diurnal rainfall amplitudes.

Moisture flux convergence

The vertically integrated moisture flux convergence ($-\nabla\cdot Q$) was calculated based on Eqs. (4)–(6), using the data from ERA5[43].

$$Q_\lambda = \frac{1}{g}\int_{500\mathrm{hPa}}^{1000\mathrm{hPa}} qu\, dp, \quad (4)$$

$$Q_\varphi = \frac{1}{g}\int_{500\mathrm{hPa}}^{1000\mathrm{hPa}} qv\, dp, \quad (5)$$

$$-\nabla\cdot Q = -\left(\frac{\partial Q_\lambda}{\partial \mathrm{x}} + \frac{\partial Q_\varphi}{\partial \mathrm{y}}\right), \quad (6)$$

where g, q, p, u, and v represent the gravitational acceleration, specific humidity, pressure, zonal wind, and meridional wind, respectively. Q_λ and Q_φ represents the zonal and meridional components of the vertically integrated moisture flux vector, respectively.

Data availability

The RMM index data is publicly available at http://www.bom.gov.au/climate/mjo/. The dataset of IMERG[42] and ERA5[43] can be accessed online at https://disc.gsfc.nasa.gov/datasets/GPM_3IMERGHH_06/summary and https://cds.climate.copernicus.eu/cdsapp#!/dataset/reanalysis-era5-pressure-levels?tab=overview, respectively.

Code availability

The data in this study was analyzed, and all the figures in the manuscript were created using the Grid Analysis and Display System (GrADS) Version 2.1.1. To access the GrADS software, please visit http://cola.gmu.edu/grads/downloads.php. All relevant codes used in this work are not publicly available but can be made available to qualified researchers upon reasonable request from the corresponding author.

Received: 27 July 2023; Accepted: 31 January 2024;
Published online: 12 February 2024

References

1. Madden, R. A. & Julian, P. R. Detection of a 40–50 Day Oscillation in the Zonal Wind in the Tropical. *Pacific. J. Atmos. Sci.* **28**, 702–708 (1971).
2. Madden, R. A. & Julian, P. R. Description of Global-Scale Circulation Cells in the Tropics with a 40–50 Day. *Period. J. Atmos. Sci.* **29**, 1109–1123 (1972).
3. Zhang, C. Madden-Julian Oscillation. *Rev. Geophys.* **43**, RG2003 (2005).
4. Pai, D. S., Bhate, J., Sreejith, O. P. & Hatwar, H. R. Impact of MJO on the intraseasonal variation of summer monsoon rainfall over India. *Clim. Dyn.* **36**, 41–55 (2011).
5. Hendon, H. H. & Salby, M. L. The life cycle of the Madden-Julian. *Oscillation. J. Atmos. Sci.* **51**, 2225–2237 (1994).
6. Adames, Á. F., Wallace, J. M. & Monteiro, J. M. Seasonality of the structure and propagation characteristics of the MJO. *J. Atmos. Sci.* **73**, 3511–3526 (2016).
7. Dasgupta, P. et al. Interannual variability of the frequency of MJO phases and its association with two types of ENSO. *Sci. Rep.* **11**, 11541 (2021).
8. Suematsu, T. & Miura, H. Changes in the Eastward Movement Speed of the Madden–Julian Oscillation with Fluctuation in the Walker Circulation. *J. Clim.* **35**, 211–225 (2022).
9. Rauniyar, S. P. & Walsh, K. J. E. Scale Interaction of the diurnal cycle of rainfall over the maritime continent and Australia: influence of the MJO. *J. Clim.* **24**, 325–348 (2011).
10. Oh, J. H., Kim, K. Y. & Lim, G. H. Impact of MJO on the diurnal cycle of rainfall over the western Maritime Continent in the austral summer. *Clim. Dyn.* **38**, 1167–1180 (2012).
11. Peatman, S. C., Matthews, A. J. & Stevens, D. P. Propagation of the Madden–Julian oscillation through the maritime continent and scale interaction with the diurnal cycle of precipitation. *Q. J. R. Meteorol. Soc.* **140**, 814–825 (2014).
12. Dias, J., Sakaeda, N., Kiladis, G. N. & Kikuchi, K. Influences of the MJO on the space-time organization of tropical convection. *JGR Atmos.* **122**, 8012–8032 (2017).
13. Schreck, C. J. Global Survey of the MJO and Extreme Precipitation. *Geophys. Res. Lett.* **48**, e2021GL094691 (2021).
14. Bui, H. X., Maloney, E. D., Short, E. & Riley Dellaripa, E. M. Diurnal cycle of wind speed and precipitation over the northern Australia coastal region: CYGNSS observations. *Geophys. Res. Lett.* **50**, e2023GL103005 (2023).

15. Prajwal, K., Kottayil, A. & Xavier, P. Impact of Madden Julian Oscillation on the diurnal cycle of precipitation over the west coast of India. *Atmos. Res.* **278**, 106343 (2022).
16. Lopez-Bravo, C., Vincent, C. L., Huang, Y. & Lane, T. P. The diurnal cycle of rainfall and deep convective clouds around Sumatra and the associated MJO-induced variability during Austral Summer in Himawari-8. *JGR Atmos.* **128**, e2023JD039132 (2023).
17. Jayawardena, I. M. S. P., Wheeler, M. C., Sumathipala, W. L. & Basnayake, B. R. S. B. Impacts of the Madden-Julian Oscillation (MJO) on rainfall in Sri Lanka. *Mausam* **71**, 405–422 (2020).
18. Barnes, H. C. & Houze, R. A. Precipitation hydrometeor type relative to the mesoscale airflow in mature oceanic deep convection of the Madden-Julian. *Oscillation. J. Geophys. Res. Atmos.* **119**, 13990–14014 (2014).
19. Rowe, A. K. & Houze, R. A. Cloud organization and growth during the transition from suppressed to active MJO. *conditions. J. Geophys. Res. Atmos.* **120**, 10324–10350 (2015).
20. Jayawardena, I., Sumathipala, W. L. & Basnayake, B. Impact of Madden Julian oscillation (MJO) and other meteorological phenomena on the heavy rainfall event from $19^{th} - 28^{th}$ December, 2014 over Sri Lanka. *J. Natl. Sci. Found. Sri Lanka* **45**, 101–111 (2017).
21. Liang, S., Wang, D., Ziegler, A. D., Li, L. Z. X. & Zeng, Z. Madden–Julian Oscillation-induced extreme rainfalls constrained by global warming mitigation. *npj Clim. Atmos. Sci.* **5**, 67 (2022).
22. Ichikawa, H. & Yasunari, T. Propagating diurnal disturbances embedded in the Madden-Julian Oscillation. *Geophys. Res. Lett.* **34**, L18811 (2007).
23. Anandh, P. C., Vissa, N. K. & Broderick, C. Role of MJO in modulating rainfall characteristics observed over India in all seasons utilizing TRMM. *Int. J. Climatol.* **38**, 2352–2373 (2018).
24. Zhou, Y., Wang, S. & Fang, J. Diurnal Cycle and Dipolar Pattern of Precipitation over Borneo during an MJO Event: Lee Convergence and Offshore. *Propagation. J. Atmos. Sci.* **79**, 2145–2168 (2022).
25. Fang, J. & Du, Y. A global survey of diurnal offshore propagation of rainfall. *Nat. Commun.* **13**, 7437 (2022).
26. Zhu, B., Du, Y. & Gao, Z. Influences of MJO on the Diurnal Variation and Associated Offshore Propagation of Rainfall near Western Coast of Sumatra. *Atmosphere* **13**, 330 (2022).
27. Tian, B., Waliser, D. E. & Fetzer, E. J. Modulation of the diurnal cycle of tropical deep convective clouds by the MJO. *Geophys. Res. Lett.* **33**, L20704 (2006).
28. Barrett, B. S., Densmore, C. R., Ray, P. & Sanabia, E. R. Active and weakening MJO events in the Maritime Continent. *Clim. Dyn.* **57**, 157–172 (2021).
29. Mishra, S., Sahany, S. & Salunke, P. Linkages between MJO and summer monsoon rainfall over India and surrounding region. *Meteorol. Atmos. Phys.* **129**, 283–296 (2017).
30. Ichikawa, H. & Yasunari, T. Time–Space Characteristics of Diurnal Rainfall over Borneo and Surrounding Oceans as Observed by TRMM-PR. *J. Clim.* **19**, 1238–1260 (2006).
31. Huang, W.-R., Koralegedara, S. B., Tung, P.-H. & Chiang, T.-Y. Seasonal changes in diurnal rainfall over Sri Lanka and possible mechanisms. *Atmos. Res.* **286**, 106692 (2023).
32. Knutson, T. R. & Weickmann, K. M. 30–60 Day Atmospheric Oscillations: Composite Life Cycles of Convection and Circulation Anomalies. *Mon. Weather Rev.* **115**, 1407–1436 (1987).
33. Salby, M. L. & Hendon, H. H. Intraseasonal Behavior of Clouds, Temperature, and Motion in the Tropics. *J. Atmos. Sci.* **51**, 2207–2224 (1994).
34. Zhang, C. & Dong, M. Seasonality in the Madden–Julian Oscillation. *J. Clim.* **17**, 3169–3180 (2004).
35. Benedict, J. J. & Randall, D. A. Observed Characteristics of the MJO Relative to Maximum Rainfall. *J. Atmos. Sci.* **64**, 2332–2354 (2007).
36. Golding, B. W. A Numerical Investigation of Tropical Island Thunderstorms. *Mon. Weather Rev.* **121**, 1417–1433 (1993).
37. Lu, J., Li, T. & Wang, L. Precipitation diurnal cycle over the Maritime Continent modulated by the MJO. *Clim. Dyn.* **53**, 6489–6501 (2019).
38. Tan, H. et al. Understanding the role of topography on the diurnal cycle of precipitation in the Maritime Continent during MJO propagation. *Clim. Dyn.* **58**, 3003–3019 (2022).
39. Vincent, C. L. & Lane, T. P. Evolution of the diurnal precipitation cycle with the passage of a Madden–Julian Oscillation event through the Maritime Continent. *Mon. Weather Rev.* **144**, 1983–2005 (2016).
40. Huang, W.-R., Chang, Y.-H., Deng, L. & Liu, P.-Y. Simulation and Projection of Summer Convective Afternoon Rainfall Activities over Southeast Asia in CMIP6 Models. *J. Clim.* **34**, 5001–5016 (2021).
41. Huang, W.-R., Chien, Y.-T., Cheng, C.-T., Hsu, H.-H. & Koralegedara, S. B. The Role of Sea Surface Temperature in Shaping the Characteristics of Future Convective Afternoon Rainfall in Taiwan. *npj Clim Atmos Sci* **6**, 198 (2023).
42. Huffman, G. J. et al. in *Satellite Precipitation Measurement. Advances in Global Change Research Vol. 67 Advances in Global Change Research* (eds V. Levizzani et al.) 19, 343–353 (Springer, Cham, 2020).
43. Hersbach, H. et al. The ERA5 global reanalysis. *Q. J. Roy. Meteorol. Soc.* **146**, 1999–2049 (2020).
44. Wheeler, M. C. & Hendon, H. H. An all-season real-time multivariate MJO index: Development of an index for monitoring and prediction. *Mon. Weather Rev.* **132**, 1917–1932 (2004).
45. Jeong, J.-H., Kim, B.-M., Ho, C.-H. & Noh, Y.-H. Systematic Variation in Wintertime Precipitation in East Asia by MJO-Induced Extratropical Vertical Motion. *J. Clim.* **21**, 788–801 (2008).
46. Diamond, H. J. & Renwick, J. A. The climatological relationship between tropical cyclones in the southwest pacific and the Madden–Julian Oscillation. *Int. J. Climatol.* **35**, 676–686 (2014).
47. Li, W., Guo, W., Hsu, P. C. & Xue, Y. Influence of the Madden-Julian oscillation on Tibetan Plateau snow cover at the intraseasonal time-scale. *Sci. Rep.* **6**, 30456 (2016).
48. Gadelha, A. N. et al. Grid box-level evaluation of IMERG over Brazil at various space and time scales. *Atmos. Res.* **218**, 231–244 (2019).
49. Li, X., O, S., Wang, N., Liu, L. & Huang, Y. Evaluation of the GPM IMERG V06 products for light rain over Mainland China. *Atmos. Res.* **253**, 105510 (2021).
50. Moazami, S., Na, W., Najafi, M. R. & de Souza, C. Spatiotemporal bias adjustment of IMERG satellite precipitation data across Canada. *Adv. Water Resour.* **168**, 104300 (2022).
51. Huang, W.-R. et al. Summer Convective Afternoon Rainfall Simulation and Projection Using WRF Driven by Global Climate Model. Part I: Over Taiwan. *Terr. Atmos. Ocean Sci.* **27**, 659–671 (2016).
52. Huang, W.-R., Chang, Y.-H. & Huang, P.-H. Relationship between the Interannual Variations of Summer Convective Afternoon Rainfall Activity in Taiwan and SSTA(Nino3.4) during 1961-2012: Characteristics and Mechanisms. *Sci. Rep.* **9**, 9378 (2019).
53. Guillod, B. P., Orlowsky, B., Miralles, D. G., Teuling, A. J. & Seneviratne, S. I. Reconciling spatial and temporal soil moisture effects on afternoon rainfall. *Nat Commun* **6**, 6443 (2015).
54. Huang, W.-R., Liu, P.-Y., Hsu, J., Li, X. & Deng, L. Assessment of Near-Real-Time Satellite Precipitation Products from GSMaP in Monitoring Rainfall Variations over Taiwan. *Remote Sens* **13**, 202 (2021).
55. Koralegedara, S. B., Huang, W.-R., Tung, P.-H. & Chiang, T.-Y. El Niño-Southern Oscillation modulation of springtime diurnal rainfall over a tropical Indian Ocean island. *Earth Space Sci.* **10**, e2023EA002832 (2023).

Acknowledgements

This study was supported by the National Science and Technology Council of Taiwan under NSTC 112-2111-M-003-004 and NSTC 112-2625-M-003-003. Koralegedara, S.B. was supported by NSTC 112-2811-M-003-009.

Author contributions

W.R.H. designed the study. W.R.H. and T.Y.C. performed the major analysis with assistance from other co-authors. All authors aided in the interpretation of results and contributed to reviewing and editing, with W.R.H. and S.B.K. leading the initial draft. All authors read and approved the final manuscript.

Competing interests

The authors declare no competing interests.

Additional information

Supplementary information The online version contains supplementary material available at https://doi.org/10.1038/s41612-024-00586-5.

Correspondence and requests for materials should be addressed to Wan-Ru Huang.

Reprints and permissions information is available at http://www.nature.com/reprints

Publisher's note Springer Nature remains neutral with regard to jurisdictional claims in published maps and institutional affiliations.

Open Access This article is licensed under a Creative Commons Attribution 4.0 International License, which permits use, sharing, adaptation, distribution and reproduction in any medium or format, as long as you give appropriate credit to the original author(s) and the source, provide a link to the Creative Commons licence, and indicate if changes were made. The images or other third party material in this article are included in the article's Creative Commons licence, unless indicated otherwise in a credit line to the material. If material is not included in the article's Creative Commons licence and your intended use is not permitted by statutory regulation or exceeds the permitted use, you will need to obtain permission directly from the copyright holder. To view a copy of this licence, visit http://creativecommons.org/licenses/by/4.0/.

© The Author(s) 2024